ARTICLE

Enhanced Property of Thin Cuprous Oxide Film Prepared through Green Synthetic Route

Achraf El Kasmi[a,b*], Henning Vieker[d], Ling-nan Wu[a], André Beyer[d], Tarik Chafik[b], Zhen-yu Tian[a,c*]

a. Institute of Engineering Thermophysics, Chinese Academy of Sciences, Beijing 100190, China
b. Laboratory LGCVR UAE/L01FST, University Abdelmalek Essaadi, Tangier B.P. 416, Morocco
c. University of Chinese Academy of Sciences, Beijing 100049, China
d. Department of Physics, Bielefeld University, Universitätsstraße 25, D-33615 Bielefeld, Germany

(Dated: Received on December 10, 2018; Accepted on March 22, 2019)

Thin cuprous oxide films have been prepared by chemical vapor deposition (pulsed spray evaporation-chemical vapor deposition) method without post-treatment. The synthesis of cuprous oxide was produced by applying a water strategy effect. Then, the effect of water on the morphology, topology, structure, optical properties and surface composition of the obtained films has been comprehensively investigated. The results reveal that a pure phase of Cu_2O was obtained. The introduction of a small quantity of water in the liquid feedstock lowers the band gap energy from 2.16 eV to 2.04 eV. This finding was mainly related to the decrease of crystallite size due to the effect of water. The topology analyses, by using atomic force microscope, also revealed that surface roughness decreases with water addition, namely more uniform covered surface. Moreover, theoretical calculations based on density functional theory method were performed to understand the adsorption and reaction behaviors of water and ethanol on the Cu_2O thin film surface. Formation mechanism of the Cu_2O thin film was also suggested and discussed.

Key words: Cuprous oxide thin films, Pulsed spray evaporation-chemical vapor deposition method, Green synthetic route, Optical and topology property, Band gap, Density functional theory calculation

I. INTRODUCTION

Transition metal oxides have caught great attention in the past decades in terms of their promising properties for a variety of applications [1–5]. As one of the various metal oxides, cuprous oxide is an attractive material regarding its application when combined with its major interesting characteristics such as low-cost, abundant availability, and nontoxic nature [6–9]. Cuprous oxide material has been considered as one of the most promising materials in different applications, *e.g.*, batteries of lithium-ion [10, 11], photocatalysis [12–14], and photovoltaic cells [4, 15]. Taking into account that it is a p-type semiconductor with a band gap energy (E_g) of 2.17 eV [16, 17], cuprous oxide thin film has been regarded as a potential material for solar cells, because of its high absorption coefficient in the visible region [18, 19]. Moreover, by considering the sensitivity of E_g to the application of semiconductor, a slight change in E_g can lead to a promising material based on cuprous oxide for the development of semiconductors.

Several advanced methods have been employed to prepare cuprous oxide thin films, including sol-gel [20, 21], sputtering [22, 23], electrodeposition [24–26], pulsed laser deposition [15, 27], and atomic layer deposition [28], *etc.* However, those methods could yield a mixture of CuO/Cu_2O crystalline phases and transformation of phases especially at high temperature [29–31]. Moreover, cuprous oxide was generally prepared by either using surfactant [24, 32, 33] or reducing agents [34]. To the best of our knowledge, the direct preparation of pure cuprous oxide has been scarcely reported in the literature. Thus, in order to overcome such difficulties in synthesizing Cu_2O, an appropriate synthesis method is needed.

At this regard, pulsed-spray evaporation chemical vapor deposition (PSE-CVD), as a simple, easy and low-cost technique with other attractive advantages [35–37], has recently attracted much attention in thin film deposition of Co-, Cu- and Mn-based oxides with high purity [36, 38–41]. Particularly, the band gap characteristic, one of the important properties involving absorption intensity of sunlight for semiconductors, can be tuned via PSE-CVD [42–45]. Recently, Baeumer *et al.* have investigated the effect of water on the thin film composition and growth kinetics, and found that the water has a beneficial effect and strongly depending on the concentration of water in the feedstock [46]. In additi-

*Authors to whom correspondence should be addressed. E-mail: tianzhenyu@iet.cn, achraf@iet.cn

on, in our previous work, the involvement of water in the preparation provided a very good effect on the catalytic performance of CO [47]. Therefore, using water in the PSE-CVD process to tune optical properties is expected to exhibit a great potential in preparing cuprous oxide material.

In present work, we aim to synthesize pure crystalline cuprous oxide thin films at low temperature via PSE-CVD and reveal the effect of water contained in the feedstock on the control of Cu_2O thin film properties. Comprehensive analyses have been used to highlight the effect of water on the crystalline structure, topology, surface morphology, chemical composition, and optical property of cuprous oxide thin films. Based on the experimental observations, the relationship among the effect of water, E_g and crystallite size was correlated. In addition, theoretical calculations based on DFT method were also performed to understand the adsorption and reaction behaviors on Cu_2O thin film surface during film formation. Attention was also given to the discussion of the formation mechanism of Cu_2O thin film. The results are expected to improve the applicability of the Cu_2O and other films considered for semiconductor fabrication.

II. EXPERIMENTS

The cuprous oxide thin films were synthesized in a PSE-CVD reactor with the use of $Cu(acac)_2$ precursor and ethanol solvent [47, 48]. Moreover, a novel step of adding an amount of water (2.5 vol%) to the feedstock was also investigated here. In addition, the amount of water was carefully chosen to ensure a complete dissolution of solid precursor in the liquid feedstock, because adding 10 vol% water would result in the partial dissolution of $Cu(acac)_2$ precursor. After deposition, the samples were taken out from the CVD reactor after cooling down to room temperature, because the assumed Cu_2O bulk phase might have been oxidized to CuO directly at the surface, as the sample was transported through air prior to measurements [49].

The crystalline structure of the prepared films was identified using X-ray diffraction (XRD) technique, by referring to the XRD database. The morphology of the samples was scanned by using a helium ion microscope (HIM). The surface topology of the samples was investigated by atomic force microscope (AFM, Nanosurf C3000 controller), which was operated in tapping mode at room temperature. X-ray photoelectron spectroscopy (XPS) was performed to determine the surface film composition. Ultraviolet-visible spectrometry (UV-Vis, Shimadzu UV-2501) was applied to assess the optical properties of the cuprous oxide films.

The adsorption of H_2O and ethanol on Cu_2O surface was studied by using density functional theory (DFT) calculation to understand the adsorption and reaction behaviors on Cu_2O thin film surface. Perdew-Burke-Ernzerhof (PBE) and generalized gradient approximation (GGA) were used for correlation and exchange potentials [50]. Perfect $Cu_2O(111)$ surface model was established to investigate Cu_2O surface properties as it was the most stable thermodynamically stable low-index surface of Cu_2O crystal. $Cu_2O(111)$ surface model was cleaved from a perfect Cu_2O crystal with p(2×2) surface expansion. The surface slab comprised of three Cu atomic layers and six O atomic layers, and each Cu atomic layer was sandwiched by two O atomic layers. A sheet of 12 Å vacuum layer was placed perpendicular to the surface plane in order to avoid interference from imaging surfaces. A 3×3×1 Monkhorst-Pack sampling grid was used and the atomic orbital cutoff was selected as 4.0 Å during energetic calculations. The adsorption energy (E_{ad}) of gaseous molecules on the Cu_2O (111) surface was calculated by:

$$E_{ad} = E_{sys} - E_{ads} - E_{surf} \quad (1)$$

where E_{sys} is the energy of the adsorption system after adsorption, E_{surf} is the energy of the clean surface before adsorption, and E_{ads} is adsorbate energy (either H_2O or ethanol).

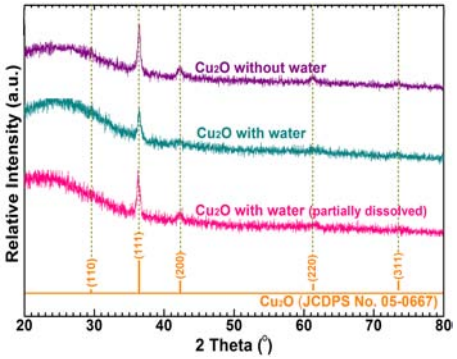

FIG. 1 XRD patterns of deposited Cu_2O films.

III. RESULTS AND DISCUSSION

A. Structure

The crystalline structure of the deposited thin films (thickness ~200 nm) was investigated by the XRD measurements, as shown in FIG. 1. It is revealed that the samples exhibit well-defined diffraction peaks of Cu_2O cubic structure (JCPDS No.05-0667), without any impurity phases, indicating that the pure cuprous oxide structure for the samples was obtained.

To determine the crystallite size of the film materials, Scherrer equation was applied to the strongest peak located at 36.42° as the preferred growth direction plane (111). Using this equation, the crystallite size was found to be (21±1) nm (without adding water), while this value tends to be reduced ((17±1) nm) when water was added to the feedstock. In an attempt to achieve the formation of the nanocrystalline structures, different researches have been performed by using surfactants

DOI:10.1063/1674-0068/cjcp1812277

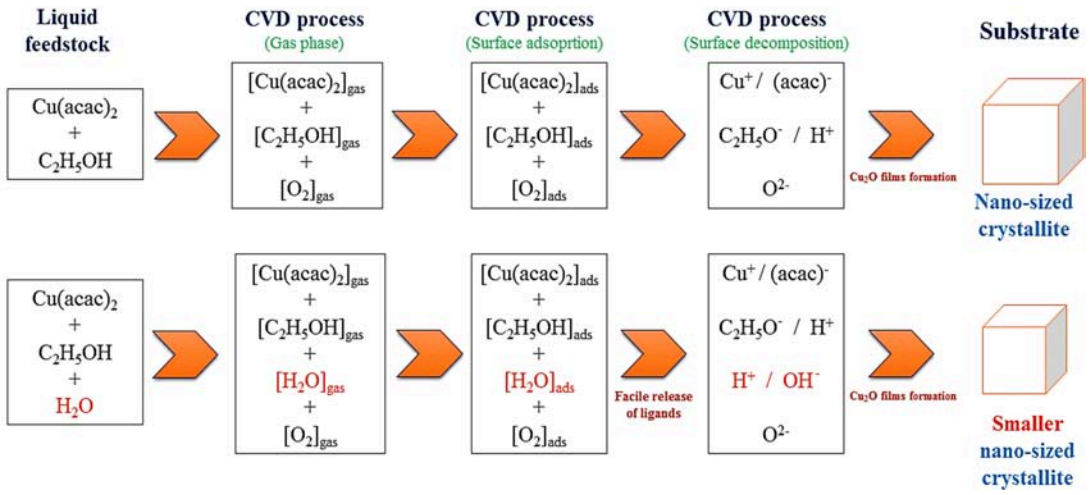

FIG. 2 Schematic of formation pathways of Cu_2O thin films in the PSE-CVD process.

[32, 33] or reducing agents [34, 51]. In addition, the formation of nanocrystalline Cu_2O is interesting for such applications, although the mechanism is not so clear yet. Here, it is worth mentioning that the formation of nanocrystalline structures of Cu_2O was achieved without utilizing any surfactants or reduction agents, which reflects the synergistic effect of using PSE-CVD for synthesizing Cu_2O. Moreover, the reduction of crystallite size by the strategy of water addition is suggested to be linked to the generation of new species by changing the formation pathway reactions during deposition process that leads inconsequently to thermodynamically much stable condition of synthesis, which in turn permits to form much smaller Cu_2O nanocrystalline, as proposed in the FIG. 2. In accordance with Pinkas *et al.* [52], the presence of water in the deposition process could lead to an easy release of free acac ligands from the $Cu(acac)_2$, which could be activated by a proton transfer from the coordinated water. It was reported that water dissociation at the surface Cu_2O films after its binding to the Cu surface turned to form -OH species that will be embedded in the film formation [53]; thus, that the involvement of water in Cu_2O synthesis could further contribute to stabilizing the Cu_2O defects and by the consequent result in enhanced physicochemical properties. Also, it is worthly pointing out that the nanocrystal size can be controlled by adjusting the content of water in the feedstock, with ensuring that the solid precursor is completely dissolved in the feedstock. As reported, the nanocrystalline materials with small sizes have a high photocatalytic efficiency because of its unique properties conferred by the small physical dimensions [54]. Accordingly, the effect of content of water on the crystallite size may affect the physicochemical properties and further could contribute to improving the performance of the prepared films destined to photocatalytic and photovoltaic applications.

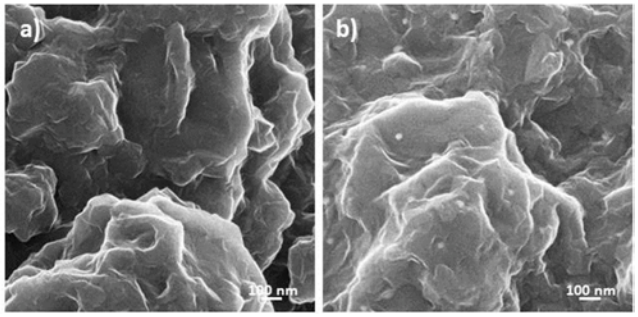

FIG. 3 Cu_2O films images (a) without H_2O and (b) with H_2O.

B. Morphology and topography

Helium ion microscopy (HIM) was performed in the present work to investigate the morphology of Cu_2O films. Images of Cu_2O thin films are shown in FIG. 3. The micrographs show an agglomeration of the nanocrystals. Moreover, both deposited films show porous and open structures, whereas the one with addition of water exhibits a less porous and open structure. Recently, it was reported that high photovoltaic performance is well correlated with the decrease in grain boundaries [55]; in accordance, the further agglomeration (in the case of adding water) of nanocrystals with less porous and open structure characteristic found in the present work could be advantageous for semiconductors.

Additionally, the water added into the feedstock results in further losing the shape of the nanocrystals, as shown in FIG. 3(b), and this behaviour may be due to the decrease in nanocrystalline size, as revealed by the XRD analysis. The observed decrease in the crystallite size, in the case of water addition, could be due to new generated species (*e.g.*, -OH) resulting from water dissociation at the surface of the Cu_2O films during deposi-

DOI:10.1063/1674-0068/cjcp1812277

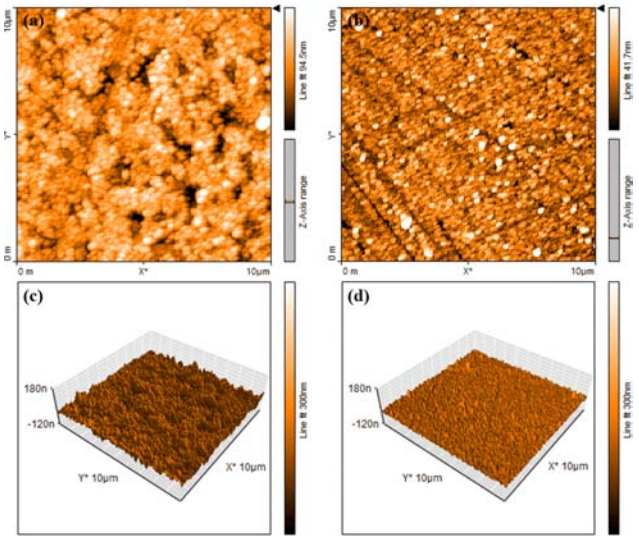

FIG. 4 AFM images of Cu_2O films deposited on bare glass: (a, c) without H_2O and (b, d) with H_2O.

tion [6], and as a consequence could control the growth orientation of Cu_2O crystallite. The latter leads to a smaller nanocrystalline structure because the structure of the nanocrystal is thermodynamically much stable under the adopted synthesis conditions (FIG. 2). Moreover, the chemical surface analysis of the prepared films using XPS (as will be shown in the following section) confirmed that there are more oxygen species adsorbed on the surface. Nevertheless, it could be deduced that the content of water in the system may affect the properties of the prepared films and would further benefit to their properties.

To investigate the surface topology of the deposited cuprous oxide thin films, AFM technique was performed. FIG. 4 shows two-dimensional (2D) and three-dimensional (3D) topographical images of both deposited films. The obtained images confirm the agglomeration of small nanocrystals that are previously observed by HIM. From AFM images, it can be seen that films deposited by adding water are more densely packed with smaller regular shaped grains than those observed in films deposited without adding water. Moreover, we can clearly observe some voids and lacks in samples deposited without water; while films tend to be more homogeneous and continuously covered on the substrate in the case of adding water, with some microcrack lines that might be attributed to the simultaneous multi-layer growth mode happening during the deposition processes. It may also reflect that water increased the surface tension of the smaller obtained grains to further form a continuous film material. Accordingly, it was reported that the decrease in grain boundaries is much appropriate for solar cells [55]. Moreover, the surface roughness of both deposited samples is determined by two main parameters: mean roughness (R_a) and root mean square roughness (R_g) within an area of

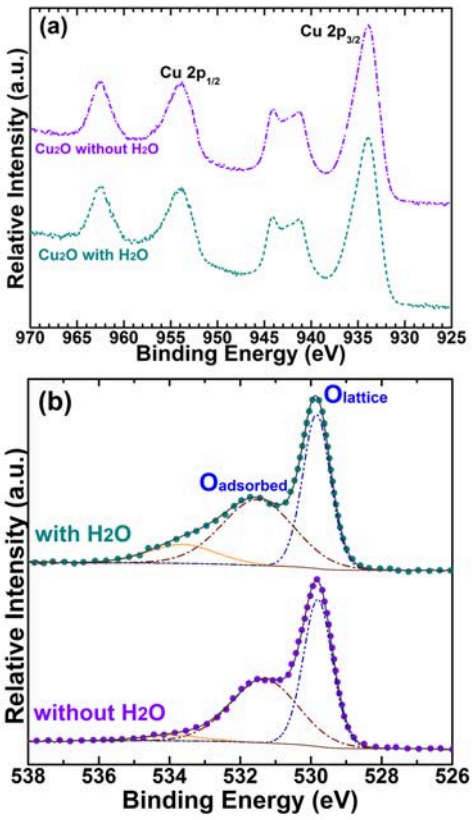

FIG. 5 XPS spectra of (a) Cu 2p and (b) O 1s for Cu_2O thin films.

10 µm×10 µm. The values of R_a and R_g for Cu_2O films deposited without water are 13.38 nm and 16.45 nm, respectively; while these values tend to decrease when water was added, to 6.08 nm and 7.85 nm for R_a and R_g, respectively. Thus, the content of water results in decreasing the roughness values that lead to depositing films with a smoother surface than in the case of depositing sample without water, which again confirms the observed results by HIM. Hence, the topographical studies reveal that the Cu_2O films deposited by adding water strategy lead to forming films which are less rough and more uniformly covered the surface, which in turn exhibit that content of water plays an important role during the film formation process that can offer an advantage for solar cell and semiconductor application.

C. Chemical composition

To better investigate the chemical composition of the prepared films, XPS measurements were carried out. XPS results revealed the existence of Cu and O spectra in both films (FIG. 5). The Cu 2p spectrum shows the presence of two peaks of Cu $2p_{1/2}$ and Cu $2p_{3/2}$ at ∼954 and ∼934 eV (FIG. 5(a)). The Cu 2p spectrum may show the structure of CuO and/or $Cu(OH)_2$ that partially formed at the surface of Cu_2O due to the oxidation of the prepared samples when taken out from

DOI:10.1063/1674-0068/cjcp1812277

CVD reactor after preparation. The spectrum of O 1s exhibits the presence of two peaks, as shown in FIG. 5(b). The one located at ∼530 eV is characteristic of lattice oxygen species bound to copper [56], while the one at higher binding energy (BE) is attributed to the presence of different adsorbed oxygen species and hydroxyl species as shown from deconvolution.

Compared to the sample prepared without water, the amount of adsorbed oxygen species at the surface increases in the case of adding water into the feedstock, as indicated in FIG. 5(b). Thus, these results confirm that the content of water in the feedstock leads to additional oxygen species generated at the surface. Accordingly, the generation of the additional amount of oxygen at the surface when water is added into the feedstock can confirm that additional reactions occurred during the deposition process leading to the generation of new species. Thus, these reactions engendered by the water addition can be responsible for the change occurring in the crystallite size through changing the formation pathway reactions during the film deposition process, as proposed in FIG. 2. Moreover, this change in the crystalline size, with keeping the same crystalline structure, could further reflect on its properties, *e.g.* optical properties.

D. Optical property

Metal oxides with low E_g have been reported to exhibit good performance [57]. To investigate the optical properties into the determination of E_g of the prepared films, the UV-visible spectra were measured in the wavelength range of 300−700 nm (FIG. 6(a)). The E_g of the both deposited films were derived from Tauc's equation:

$$\alpha h\nu = A(h\nu - E_g)^r \quad (2)$$

FIG. 6(b) shows the Tauc plots of $(\alpha h\nu)^2$ versus $h\nu$ for the both deposited films, which permits to determine the E_g values [58]. The value of E_g for the sample deposited without water is found to be 2.16 eV, which is in line with previously reported data for the same oxide [16, 17]. Furthermore, it is of interest to point out that E_g shifts towards a lower value for the sample prepared with water, indicating that the water addition strategy led to shifting E_g. Lastly, many efforts were devoted to lowing the band gap energy for low-cost solar cell materials [59–61]. Also, several studies reported the influence of parameters on the E_g, the results are given in Table I. Compared to these results and considering the optimal band gap for the band solar cells, the finding improvement in E_g can lead to providing a promising Cu_2O material for the development of band solar cells. Here, the mechanism of decreasing in E_g with water strategy could result from the generation of such new species that influence the formation kinetics of the thin films during the deposition process (FIG. 2).

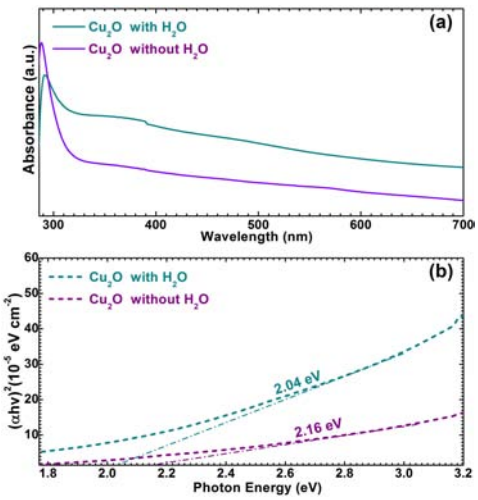

FIG. 6 (a) Optical absorption spectra and (b) Tauc's plots of cuprous oxide films.

TABLE I Comparison of the bandgap energy (E_g) of Cu_2O prepared with different methods.

Preparation method	E_g/eV
PSE-CVD (this work)	2.04−2.16
High pressure gas sputtering	2.10 [69]
Reactive magnetron sputtering	2.05−2.4 [70]
Radio frequency magnetron sputtering	2.36 [71]
Radio frequency magnetron sputtering	2.15−2.40 [72]
Activated reactive evaporation	2.00−2.60 [73]
Chemical deposition	2.10 [74]
Aqueous solution route	2.42 [75]
Electrodeposition	1.69−2.03 [76]
Electrodeposition	2.10 [77]
Oxidation of vacuum evaporated metal layers	2.32 [78]
Reductive route based ligands	1.71−2.44 [79]
Reductive conversion	2.40−2.17 [80]
Augmented-spherical-wave (ASW)	2.17 [17]
Sol-gel-like dip technique	2.10 [20]

Moreover, it was recently reported that optical proprieties of Cu_2O are related to geometrical parameter [62], also to the size of particles [6]; and the decrease in the E_g is attributed to the increase in the grain size and the structural modification of the material [63]. In the present work, the E_g value tends to decrease with the grain size, coverage discontinuity, and the substrate surface roughness. Thus, this finding of decreasing E_g is expected to be due to the decrease in grain boundaries [55] as a result of effect of water on the Cu_2O film materials.

Furthermore, to better understand the adsorption and reaction behaviors on the Cu_2O thin film surface

DOI:10.1063/1674-0068/cjcp1812277

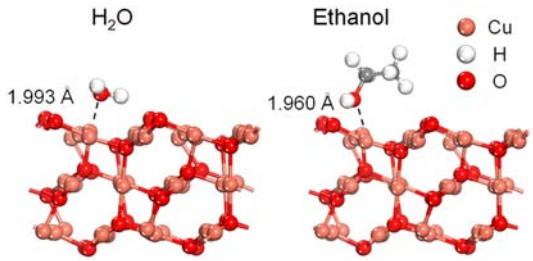

FIG. 7 Stable adsorption structures of H_2O and ethanol on $Cu_2O(111)$ surface.

(FIG. 7), the theoretical calculation was performed using DFT method. $Cu_2O(111)$ surface model was chosen to study surface reaction mechanism, because it is the most stable non-polar low-index surface of Cu_2O crystal and $Cu_2O(111)$ peak exhibited by XRD characterization as the preferred growth plane of Cu_2O, also $Cu_2O(111)$ surface is widely used as the model surface of Cu_2O catalyst [64–66]. The adsorption energy values of H_2O and ethanol on Cu_2O surface are 1.030 eV and 1.159 eV, respectively. The two values are quite similar, which means that H_2O and ethanol compete for each other in the deposition processes. The partial density of states (PDOS) analysis of H_2O and ethanol adsorption on $Cu_2O(111)$ surface Cu site is shown in FIG. 8. The results revealed that the surface one-fold Cu site is the favorable site for both of the adsorption cases. For H_2O adsorption, the p-orbital electron states of O from H_2O have a certain overlap with those of the d orbital of the surface Cu site from −8 eV to Fermi level, implying a weak covalent bond is formed between H_2O and surface Cu after adsorption. Similarly, for ethanol adsorption, there are also electron states overlapped between the p orbital of O from ethanol and the d orbital of surface Cu site for the same energy range, which indicates a weak covalent bond between ethanol and surface Cu site after adsorption. Moreover, since the outer electronic configuration of Cu^+ is $3d^{10}$, so there is no Cu 4sp distribution for Cu^+ site of $Cu_2O(111)$ surface that was confirmed by Padama *et al.* [67], and the d orbital was responsible for the surface activity of $Cu_2O(111)$ surface. Our PDOS analysis also showed that d orbitals play the dominant role in the surface activity of $Cu_2O(111)$ surface, which contributes to the majority of the electron states near the Fermi energy, and the distributions of s and p orbitals near Fermi energy are negligible. Comparatively, electron states of ethanol and the surface have a better match than H_2O and the surface, which is consistent with the adsorption energy that ethanol adsorption on the $Cu_2O(111)$ surface is a little bit stronger than H_2O. From the findings, it can be deduced that a competition in adsorption between H_2O and ethanol can occur on Cu_2O surface during film formation, which further leads to changing the reaction pathways of forming Cu_2O with different physicochemical properties.

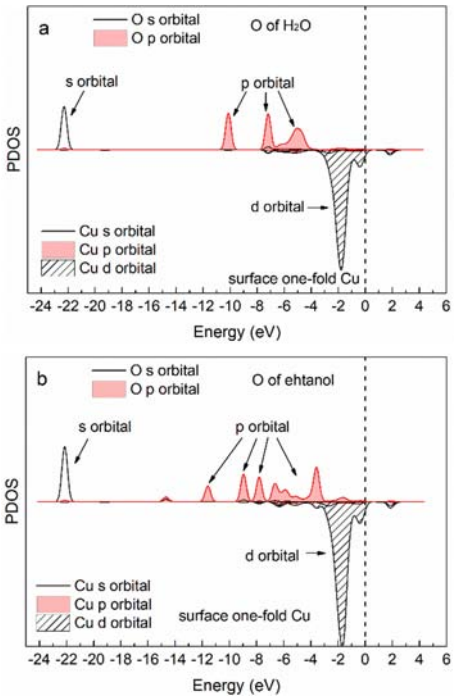

FIG. 8 PDOS analysis of (a) H_2O and (b) ethanol adsorption on $Cu_2O(111)$ surface.

Effectively, our results of controlling the band gap energy by water effect strategy with keeping the similar crystalline structure of Cu_2O (as revealed above by XRD) can be an advantageous and an alternative strategy to target the optimal E_g for desired materials and could further response to their challenged demands, *e.g.* those destined to photovoltaic cells [4, 68], instead of using some chemical additives and/or doped elements that can result sometimes in unwanted material performance. Therefore, the current finding is promising and should be explored to provide the framework for future studies in improving the performance characteristics of the low-cost materials, particulars, those destined to solar cells and semiconductor applications. Also, the use of the same approach for depositing another kind of transition metal oxides, and additional tests as power conversion efficiency can be investigated in the next study.

IV. CONCLUSION

Nanocrystalline thin films of cuprous oxide were easily prepared with the PSE-CVD method at low-deposition temperature. The green strategy of depositing thin films using water was adopted here, which resulted in the same structure of Cu_2O. When water was involved in the deposition, the crystallite size of the films decreased. The prepared films showed that the particles are partially embedded in the matrix, while the introduction of water would result in further loss of the structure by agglomeration phenomena. The topol-

DOI:10.1063/1674-0068/cjcp1812277

ogy analyses revealed that surface roughness decreases with water addition, namely more uniform covered surface. Moreover, the involvement of water resulted in a decrease in the band gap energy, whereas the amount of adsorbed oxygen species was observed to increase in the case of adding water to the feedstock. These findings indicate that the content of water in the feedstock leads to new species generated in the deposition processes involved in the chemical phase reactions, thus can further affect the optical properties towards crystallite size variation. Furthermore, theoretical calculations using DFT method revealed that the adsorption energies of H_2O and ethanol on Cu_2O surface are quite close, which permits the adsorption competition between H_2O and ethanol on Cu_2O surface during film formation, and hence change the reaction pathways of forming Cu_2O and affect physicochemical properties. Thus, the combination of PSE-CVD with the effect of water could establish a novel and alternative way to develop nanocrystalline materials by tuning the surface optical properties for applications such as solar cells as well as semiconductors.

V. ACKNOWLEDGEMENTS

This work was supported by the Ministry of Science and Technology of China (No.2017YFA0402800), the National Natural Science and Technology of China (No.91541102 and No.51476168) and Recruitment Program of Global Youth Experts. Dr. Achraf El Kasmi would kindly acknowledge the support by Chinese Academy of Sciences for Senior International Scientists within President's International Fellowship Initiative (PIFI) program, and Deutscher Akademischer Austauschdienst (DAAD) for the financial support during his Ph.D. research stay at Bielefeld University as well as the National Scientific and Technique Research Center (CNRST) for his Excellency Ph.D. Fellowship. The authors are grateful to Profs. Katharina Kohse-Höinghaus and Armin Gölzhäuser for access to their infrastructures in Bielefeld where a part of the work was performed. The Moroccan institute of IRESEN is acknowledged for the financial support (Innowind13 Nanolubricant).

[1] C. Wadia, A. P. Alivisatos, and D. M. Kammen, Environ. Sci. Technol. **43**, 2072 (2009).
[2] Z. Q. Sun, T. Liao, Y. H. Dou, S. M. Hwang, M. S. Park, L. Jiang, J. H. Kim, and S. X. Dou, Nat. Commun. **5**, 3813 (2014).
[3] Q. B. Zhang, J. X. Wang, J. C. Dong, F. Ding, X. H. Li, B. Zhang, S. H. Yang, and K. L. Zhang, Nano Energy **13**, 77 (2015).
[4] R. N. Briskman, Sol. Energy Mater. Sol. Cells **27**, 361 (1992).
[5] P. Poizot, S. Laruelle, S. Grugeon, L. Dupont, and J. M. Tarascon, Nature **407**, 496 (2000).
[6] C. H. Kuo, C. H. Chen, and M. H. Huang, Adv. Funct. Mater. **17**, 3773 (2007).
[7] C. S. Tan, S. C. Hsu, W. H. Ke, L. J. Chen, and M. H. Huang, Nano Lett. **15**, 2155 (2015).
[8] K. Akimoto, S. Ishizuka, M. Yanagita, Y. Nawa, G. K. Paul, and T. Sakurai, Sol. Energy **80**, 715 (2006).
[9] D. K. Zhou, Y. G. Li, P. T. Xu, N. S. McCool, L. Q. Li, W. Wang, and T. E. Mallouk, Nanoscale **9**, 75 (2017).
[10] C. Q. Zhang, J. P. Tu, X. H. Huang, Y. F. Yuan, X. T. Chen, and F. Mao, J. Alloys Compd. **441**, 52 (2007).
[11] J. C. Park, J. Kim, H. Kwon, and H. Song, Adv. Mater. **21**, 803 (2009).
[12] X. Xu, Z. H. Gao, Z. D. Cui, Y. Q. Liang, Z. Y. Li, S. L. Zhu, X. J. Yang, and J. M. Ma, ACS Appl. Mater. Interfaces **8**, 91 (2016).
[13] L. Xu, H. Y. Xu, S. B. Wu, and X. Y. Zhang, Appl. Surf. Sci. **258**, 4934 (2012).
[14] J. Azevedo, L. Steier, P. Dias, M. Stefik, C. T. Sousa, J. P. Arajo, A. Mendes, M. Graetzel, and S. D. Tilley, Energy Environ. Sci. **7**, 4044 (2014).
[15] T. Minami, Y. Nishi, and T. Miyata, J. Semicond. **37**, 014002 (2016).
[16] M. Y. Shen, T. Yokouchi, S. Koyama, and T. Goto, Phys. Rev. B **56**, 13066 (1997).
[17] J. Ghijsen, L. H. Tjeng, J. van Elp, H. Eskes, J. Westerink, G. A. Sawatzky, and M. T. Czyzyk, Phys. Rev. B **38**, 11322 (1988).
[18] I. Grozdanov, Mater. Lett. **19**, 281 (1994).
[19] B. P. Rai, Sol. Cells **25**, 265 (1988).
[20] S. C. Ray, Sol. Energy Mater. Sol. Cells **68**, 307 (2001).
[21] L. Armelao, D. Barreca, M. Bertapelle, G. Bottaro, C. Sada, and E. Tondello, Thin Solid Films **442**, 48 (2003).
[22] Y. Alajlani, F. Placido, A. Barlow, H. O. Chu, S. G. Song, S. Ur Rahman, R. De Bold, and D. Gibson, Vacuum **144**, 217 (2017).
[23] H. L. Zhu, J. Y. Zhang, C. Z. Li, F. Pan, T. M. Wang, and B. B. Huang, Thin Solid Films **517**, 5700 (2009).
[24] Y. Yang, J. Han, X. H. Ning, W. Cao, W. Xu, and L. J. Guo, ACS Appl. Mater. Interf. **6**, 22534 (2014).
[25] D. Mohra, M. Benhaliliba, M. Serin, M. R. Khelladi, H. Lahmar, and A. Azizi, J. Semicond. **37**, 103001 (2016).
[26] J. Kaur, O. Bethge, R. A. Wibowo, N. Bansal, M. Bauch, R. Hamid, E. Bertagnolli, and T. Dimopoulos, Sol. Energy Mater. Sol. Cells **161**, 449 (2017).
[27] N. Kikuchi and K. Tonooka, Thin Solid Films **486**, 33 (2005).
[28] S. W. Lee, Y. S. Lee, J. Heo, S. C. Siah, D. Chua, R. E. Brandt, S. B. Kim, J. P. Mailoa, T. Buonassisi, and R. G. Gordon, Adv. Energy Mater. **4**, 1301916 (2014).
[29] V. Figueiredo, E. Elangovan, G. Gonçalves, N. Franco, E. Alves, S. H. K. Park, R. Martins, and E. Fortunato, Phys. Status Solidi A **206**, 2143 (2009).
[30] M. Ristov, G. Sinadinovski, and I. Grozdanov, Thin Solid Films **123**, 63 (1985).
[31] Z. Y. Tian, H. J. Herrenbrück, P. M. Kouotou, H. Vieker, A. Beyer, A. Gölzhäuser, and K. Kohse-Höinghaus, Surf. Coat. Technol. **230**, 33 (2013).
[32] L. F. Gou and C. J. Murphy, Nano Lett. **3**, 231 (2003).
[33] M. H. Cao, C. W. Hu, Y. H. Wang, Y. H. Guo, C. X. Guo, and E. B. Wang, Chem. Commun. 1884 (2003).
[34] Y. Zhang, B. Deng, T. R. Zhang, D. M. Gao, and A. W. Xu, J. Phys. Chem. C **114**, 5073 (2010).
[35] P. A. Premkumar, N. S. Prakash, F. Gaillard, and N. Bahlawane, Mater. Chem. Phys. **125**, 757 (2011).
[36] P. M. Kouotou, H. Vieker, Z. Y. Tian, P. H. Tchoua

DOI:10.1063/1674-0068/cjcp1812277

Ngamou, A. El Kasmi, A. Beyer, A. Gölzhäuser, and K. Kohse-Höinghaus, Catal. Sci. Technol. **4**, 3359 (2014).
[37] P. M. Kouotou and Z. Y. Tian, Chin. J. Chem. Phys. **30**, 513 (2017).
[38] A. El Kasmi, M. Waqas, P. Mountapmbeme Kouotou, and Z. Y. Tian, J. Therm. Sci. **28**, 225 (2019).
[39] Z. Y. Tian, P. Mountapmbeme Kouotou, A. El Kasmi, P. H. Tchoua Ngamou, K. Kohse-Höinghaus, H. Vieker, A. Beyer, and A. Gölzhäuser, Proc. Combust. Inst. **35**, 2207 (2015).
[40] Z. Y. Tian, N. Bahlawane, V. Vannier, and K. Kohse-Höinghaus, Proc. Combust. Inst. **34**, 2261 (2013).
[41] G. F. Pan, A. El Kasmi, and Z. Y. Tian, ES Energy Environ. **2**, 58 (2018).
[42] Z. Y. Tian, H. Vieker, P. M. Kouotou, and A. Beyer, Faraday Discuss. **177**, 249 (2015).
[43] Y. Z. Jiang and N. Bahlawane, J. Alloys Compd. **485**, L52 (2009).
[44] Y. Z. Jiang and N. Bahlawane, Nanosci. Nanotechnol. Lett. **1**, 134 (2009).
[45] Y. Z. Jiang and N. Bahlawane, Thin Solid Films **519**, 284 (2010).
[46] T. Weiss, V. Zielasek, and M. Bäumer, Sci. Rep. **5**, 18194 (2015).
[47] A. El Kasmi, Z. Y. Tian, H. Vieker, A. Beyer, and T. Chafik, Appl. Catal. B Environ. **186**, 10 (2016).
[48] M. Waqas, P. M. Kouotou, A. E. Kasmi, Y. Wang, and Z. Y. Tian, ES Energy Environ. **1**, 67 (2018).
[49] B. Maack and N. Nilius, Thin Solid Films **651**, 24 (2018).
[50] J. P. Perdew, K. Burke, and M. Ernzerhof, Phys. Rev. Lett. **77**, 3865 (1996).
[51] Z. H. Wang, H. Wang, L. L. Wang, and L. Pan, Cryst. Res. Technol. **44**, 624 (2009).
[52] J. Pinkas, J. C. Huffman, D. V. Baxter, M. H. Chisholm, and K. G. Caulton, Chem. Mater. **7**, 1589 (1995).
[53] A. Önsten, J. Weissenrieder, D. Stoltz, S. Yu, M. Göthelid, and U. O. Karlsson, J. Phys. Chem. C **117**, 19357 (2013).
[54] L. Wu, J. C. Yu, X. C. Wang, L. Z. Zhang, and J. G. Yu, J. Solid State Chem. **178**, 321 (2005).
[55] K. Sardashti, R. Haight, T. Gokmen, W. Wang, L. Y. Chang, D. B. Mitzi, and A. C. Kummel, Adv. Energy Mater. **5**, 1402180 (2015).
[56] M. C. Biesinger, L. W. M. Lau, A. R. Gerson, and R. S. C. Smart, Appl. Surf. Sci. **257**, 887 (2010).
[57] B. Y. Jibril, React. Kinet. Catal. Lett. **86**, 171 (2005).
[58] V. Georgieva and M. Ristov, Sol. Energy Mater. Sol. Cells. **73**, 67 (2002).
[59] E. Salmani, A. Laghrissi, M. Rouchdi, E. Benchafia, H. Ez-Zahraouy, N. Hassanain, A. Mzerd, and A. Benyoussef, Sol. Energy **155**, 18 (2017).
[60] S. Bag, O. Gunawan, T. Gokmen, Y. Zhu, T. K. Todorov, and D. B. Mitzi, Energy Environ. Sci. **5**, 7060 (2012).
[61] T. K. Todorov, D. M. Bishop, and Y. S. Lee, Sol. Energy Mater. Sol. Cells **180**, 350 (2018).
[62] L. Zhang and H. Wang, ACS Nano. **5**, 3257 (2011).
[63] A. Bielański and J. Haber, Catal. Rev. **19**, 1 (1979).
[64] X. H. Yu, X. M. Zhang, S. G. Wang, and G. Feng, Appl. Surf. Sci. **343**, 33 (2015).
[65] L. N. Wu, Z. Y. Tian, and W. Qin, Int. J. Chem. Kinet. **50**, 507 (2018).
[66] B. Z. Sun, X. L. Xu, W. K. Chen, and L. H. Dong, Appl. Surf. Sci. **316**, 416 (2014).
[67] A. A. B. Padama, H. Kishi, R. L. Arevalo, J. L. V. Moreno, H. Kasai, M. Taniguchi, M. Uenishi, H. Tanaka, and Y. Nishihata, J. Phys.: Condens. Matter. **24**, 175005 (2012).
[68] W. Z. Wang, G. H. Wang, X. S. Wang, Y. J. Zhan, Y. K. Liu, and C. L. Zheng, Adv. Mater. **14**, 67 (2002).
[69] R. Chandra, P. Taneja, and P. Ayyub, Nanostructured Mater. **11**, 505 (1999).
[70] A. A. Ogwu, E. Bouquerel, O. Ademosu, S. Moh, E. Crossan, and F. Placido, J. Phys. D **38**, 266 (2005).
[71] M. Hari Prasad Reddy, J. F. Pierson, and S. Uthanna, Phys. Status Solidi A **209**, 1279 (2012).
[72] M. H. P. Reddy, A. Sreedhar, and S. Uthanna, Indian J. Phys. **86**, 291 (2012).
[73] B. Balamurugan and B. R. Mehta, Thin Solid Films **396**, 90 (2001).
[74] M. T. S. Nair, L. Guerrero, O. L. Arenas, and P. K. Nair, Appl. Surf. Sci. **150**, 143 (1999).
[75] Z. Yang, C. K. Chiang, and H. T. Chang, Nanotechnology **19**, 025604 (2008).
[76] Y. H. Jin, Q. Q. Li, G. H. Li, M. Chen, J. K. Liu, Y. Zou, K. L. Jiang, and S. S. Fan, Nanoscale Res. Lett. **9**, 7 (2014).
[77] T. D. Golden, M. G. Shumsky, Y. C. Zhou, R. A. VanderWerf, R. A. Van Leeuwen, and J. A. Switzer, Chem. Mater. **8**, 2499 (1996).
[78] G. Papadimitropoulos, N. Vourdas, V. E. Vamvakas, and D. Davazoglou, Thin Solid Films **515**, 2428 (2006).
[79] G. S. Theja, R. C. Lowrence, V. Ravi, S. Nagarajan, and S. P. Anthony, CrystEngComm **16**, 9866 (2014).
[80] Y. Chang, J. J. Teo, and H. C. Zeng, Langmuir **21**, 1074 (2005).

DOI:10.1063/1674-0068/cjcp1812277